

# Optical simulations and optimization of highly sensitive biosensor for cancer cell detection

ABDELKARIM EL MOUNCHARIH\*, RABI TAKASSA, OMAR FARKAD, ABDELAZIZ TCHENKA,  
EL ALAMI IBNOUELGHAZI, DRRISS ABOUELAOUALIM

LaMEE, Department of Physics, Faculty of Sciences Semlalia, Cadi Ayyad University,  
P.O. Box 2390, 40000 Marrakech, Morocco

\*Corresponding author: a.elmouncharih@gmail.com

In this work, using the two-dimensional finite difference time domain method, we are theoretically studying the optical properties of a two-dimensional photonic crystal biosensor based on silicon rods arranged as a square structure in an air bottom with two waveguides and a nanocavity. For this purpose, six different cells are infiltrated into the point defect. These six cells are Jurkat, HeLa, PC-12, MDA-MB-231, MCF-7, and basal cells. As a result, we have successfully detected cancer and benign cases of these cells through resonance peaks in the transmission spectrum. We evaluated the sensitivity, quality factor, detection limit, and figure of merit at different values for sensing region radius for optimization purposes. We report that we observed the maximum sensitivity of 1350 nm/RIU at 0.15  $\mu\text{m}$  for the basal cell. Finally, the proposed biosensor can be a miniaturized structure with extreme sensitivity in cancer cell detection models.

Keywords: refractive index sensor, sensitivity, cancer cells, photonic crystal, finite difference time domain (FDTD).

## 1. Introduction

Photonic crystals (PhCs) are an arrangement with a common form of dielectric materials having different refractive indexes that change periodically in one or more directions [1]. This periodicity gives them unique optical features, including creating an optical bandgap. The size of the PBG and its position in the spectrum can be adjusted by varying the refractive index contrast of dielectric materials and/or the periodicity of the structure that gives the possibility to prohibit a frequency range in one or more directions and polarization; therefore the ability to guide and manipulating the flow of light in photonic crystals [2, 3]. These properties make photonic crystals extremely useful in several applications. In particular, thanks to their properties of capturing photons and creating optical resonances highly sensitive to the presence of the biological analyte, the application of photonic crystals as biosensors has generated great interest [4-7].

Recently, PhCs have become one of many frameworks that can be used to design biosensors due to the low loss and high capacity in guidance and light control. The researchers worked on PhCs to increase the demand for detection applications. Nowadays, biosensors have drawn much attraction from researchers as it has vast applications in different fields in health care [8], food [9], water, and air quality monitoring [10, 11], then pathogen and drug discovery [12, 13], also disease detection [14, 15]. Difference schemes and configurations of optical sensing devices have been proposed and produced using various types of photonic crystal structures such as waveguides [16, 17], splitters [18], ring resonators [19-21], and cavities [22]. The many applications of PhCs in biosensing make them interesting for the implementation of different types of sensors [23-32].

According to SIEGEL *et al.* [33], 1918030 new cancer cases will be diagnosed in the United States in 2022, and 609360 people will die from cancer. Cancer is caused due to abnormal growth in the body cells. Blood cancer, adrenal gland cancer, cervical cancer, breast cancer, and skin cancer are the most common. Cancer screening equipment is needed to detect the cancer cell in a short time. For this reason, we directly measure the refractive index of cancer cells by considering blood and other liquid substances from affected parts of the human body. In that scenario, the PhCs was used for the cancer cells detection [34-36]. Thus, researchers tried to increase the sensitivity responses, the quality factor and figure of merit of the photonic crystal-based biosensor to improve the detection performance. In 2018, RAMANUJAM *et al.* [34] proposed the one-dimensional coated nanocomposite material based photonic crystal from the output spectrum using the effect of PBG to infiltrate and detect cancer cells. However, the sensitivity obtained is a minimum of 42 nm/RIU to a maximum of 43 nm/RIU. In 2022, ABDULKAREM *et al.* [35] assumed a nanodetector using a one-dimensional binary PhC with a defect layer to detect cancerous cells. The good sensitivity is calculated at optimized conditions and found as 2400.08 nm/RIU. The defect layer thickness is taken in the range of 4.966  $\mu\text{m}$  to test the human cells efficiently. Parallel, MIYAN *et al.* [36] proposed a 2D-PhC-based biosensor designed to detect three types of cancer cells. The sensitivity is calculated at optimized conditions and found as 15085 nm/RIU. This sensitivity is extremely high when compared to the most recent biosensors. But the sensing region radius is taken at 0.106  $\mu\text{m}$  which is very small.

In this article, we report on the design and simulation of a two-dimensional photonic crystal with waveguides and nanocavity that will be the basis of a biosensor miniaturized structure for cancer cell detection. In liquid form, the analytes of cancerous and normal cells have been considered at 80% and 30–70%, respectively [37]. The samples have been infiltrated into the sensing region. Two dimensional plane wave expansion (PWE) method [38] is used to calculate the band diagram of the proposed structure without defects. The biosensor operation, sensitivity, and the structure's transfer specifications are thoroughly studied using the 2D finite difference time domain (FDTD) method [36]. Also, to improve the sensing performance of the biosensor, this algorithm searches to find the radius optimums of the sensing region cited in the nanocavity which is higher than the reported value in the reported paper that proposed 2D-PhC based

biosensor. The proposed biosensor can improve the miniaturization of detection systems and the success of high performance.

## 2. Structure, theory, and model

### 2.1. Design of biosensor structure

The design of biosensor structure is based on silicon rods background wafer in air type with the square lattice shape. As we can see from Fig. 1, the proposed biosensor structure is without defects, and from Fig. 2, its band diagram, which is simulated by the PWE method; we show that for TE polarization, a square lattice photonic crystal of dielectric rods can provide a bandgap from  $0.2818 a/\lambda$  to  $0.4166 a/\lambda$ .

Then let us introduce some defects in our structure to break this bandgap region. Line or point defects can be introduced in these crystals either by removing a row of holes or adding new holes of different shapes or geometry, leading to the formation of a photonic crystal. The proposed biosensor structure is shown in Fig. 3. As can be seen,

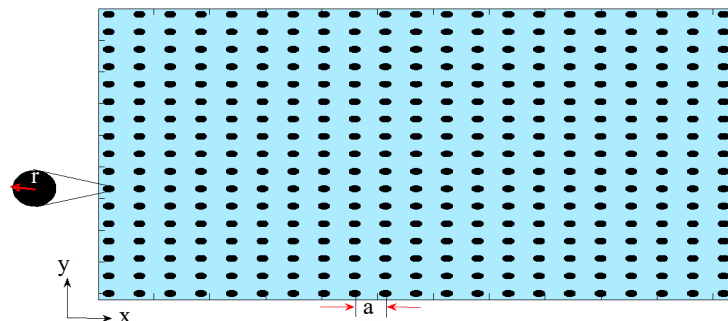


Fig. 1. Schematic of the 2D square lattice PhC structure with lattice constant  $a$  and cylinder rod radius  $r$ .

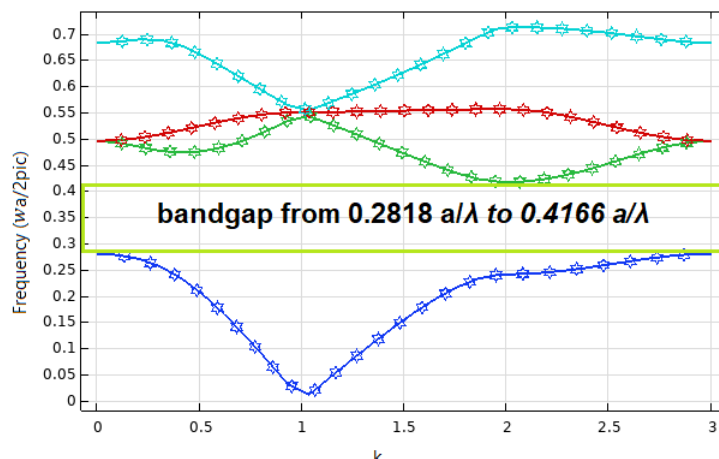


Fig. 2. Dispersion diagram of 2D-PhC structure when  $r = 0.2a$ .

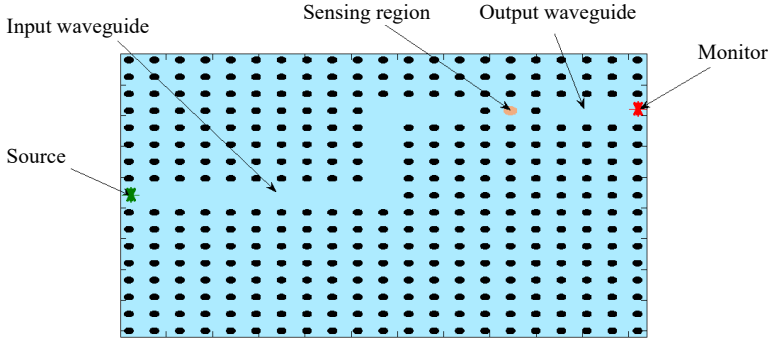


Fig. 3. Schematic of the designed PhC-based sensors containing two waveguides and one nanocavity with the radius of cylinder at sensing region  $r_s = 0.1 \mu\text{m}$ .

Table 1. Design parameters of the proposed biosensor and its values.

Parameters	Values
Configuration	Silicon rods in air
Lattice constant	$0.55 \mu\text{m}$
Rod shape	Circular
Radius of rod	$0.11 \mu\text{m}$
Lattice structure	Square
PBG range	1.3203–1.9513
Polarization	TE

the structure is not that complicated. It consists of input and output waveguides and one nanocavity usually used for cancer cell detection [36].

Table 1 gives the design parameters of the proposed biosensor structure.

## 2.2. Theory

To investigate the performance of the biosensor and the wave propagation in the proposed structure, the FDTD is applied by considering the perfectly matched layers (PML) boundary condition [39] around the simulation area. The source is located on the left of the input waveguide, and the Gaussian waves centered at 1500 nm that are stimulated by the TE mode are propagating toward the output waveguide on the right side. By monitoring the input and the output ports, the incident and the transmitted powers are calculated using Eq. (1) and the transmission coefficient of the proposed structure using Eq. (2) [40]:

$$P = \frac{1}{2} \int \operatorname{Re}(E \times H^*) ds \quad (1)$$

$$T = \frac{P_{\text{out}}}{P_{\text{int}}} \quad (2)$$

The optical detection properties of the biosensor were qualitatively estimated by sensitivity using Eq. (3), where  $\Delta\lambda$  is changing in resonant wavelength, and  $\Delta n$  is changing in refractive index [36]. The sensitivity of photonic crystal-based biosensors depends on the interaction of light with the target samples. The interaction between light and target samples in the detection region can be further affected by selecting the refractive index of the detection region.

$$S = \frac{\Delta\lambda}{\Delta n} \quad (3)$$

Also, for the proposed biosensor's resolution intensity, we used Eq. (4) to calculate the quality factor for each studied cell [36]. When the quality factor becomes too high, the filter bandwidth may be much lower than the wavelength offset caused by the manufacturing lithographic tolerances. As a result, it will lead to a complete failure of the device unless the input laser is also set. Very precise and expensive lithography is required to use these narrow band resonators (high- $Q$ ).

$$Q = \frac{\lambda_0}{\Delta\lambda} \quad (4)$$

Furthermore, the high-performance biosensor requires a low detection limit, calculated using the following equation [36]:

$$DL = \frac{FHW M}{S} \quad (5)$$

Moreover, the accuracy and precision of the proposed biosensor are obtained from the figure of merit (FOM), which is calculated using the following equation [36]:

$$FOM = \frac{S}{FHW M} \quad (6)$$

### 3. Simulation results and discussion

The results for different cells within the radius of the detection region equal to 100 nm are shown in Fig. 4. A slight shift in the resonance peak in the output transmission spectrum can be observed when the refractive index of the normal cell is substituted by the cancerous cell. Moreover, this can be checked if the cell is cancerous or benign.

For optimization purposes, we evaluated the sensitivity, quality factor, detection limit, and FOM at different values for sensing region radius. The results investigated in Figs. 5–8 show respectively the sensitivity, the quality factor, the detection limit, and the FOM of the proposed biosensor at different values for the radius of the sensing region. In all of these figures, the green line corresponds to the Jurkat cell, the red line to the PC-12 cell, the black line to the HeLa cell, the pink line to the MDA-MB-231 cell, the blue line to the MCF-7 cell, and the yellow line to basal cell.

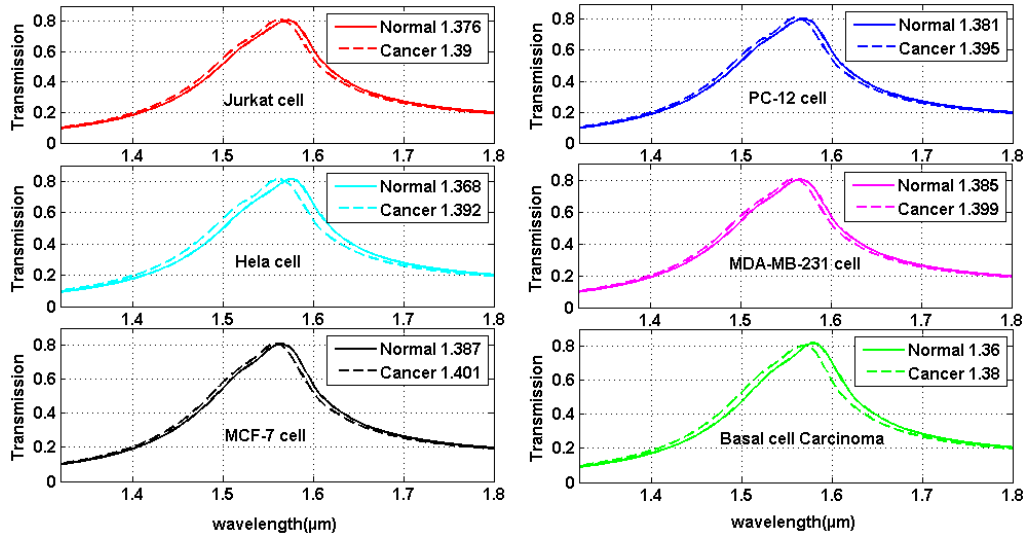


Fig. 4. The normalized transmission for different cells in both normal and cancer cases with sensing region radius equal to 100 nm.

As shown in Fig. 5, the highest sensitivity value of 1350 nm/RIU is achieved for basal cells at  $r_s = 0.14 \mu\text{m}$ , and the lowest sensitivity of 71.42 nm/RIU is observed for Jurkat and PC-12 cells at  $r_s = 0.12 \mu\text{m}$ . Also, from Fig. 6, we can see that the quality factor takes a maximum value of 15.03 for HeLa normal cell at  $r_s = 0.15 \mu\text{m}$  and a minimum value of 10.00 for MCF-7 normal cell at  $r_s = 0.10 \mu\text{m}$ . Further, the lowest value

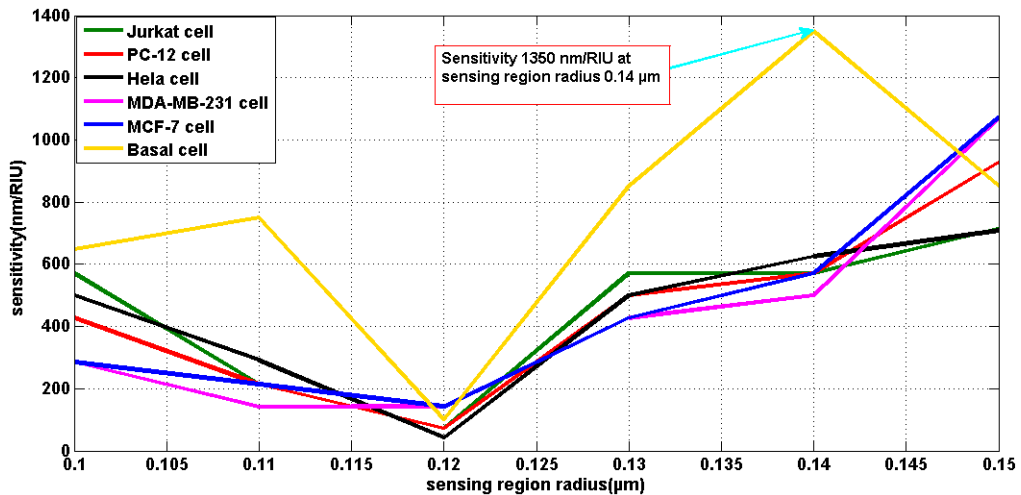


Fig. 5. Sensitivity *versus* radius of the sensing region.

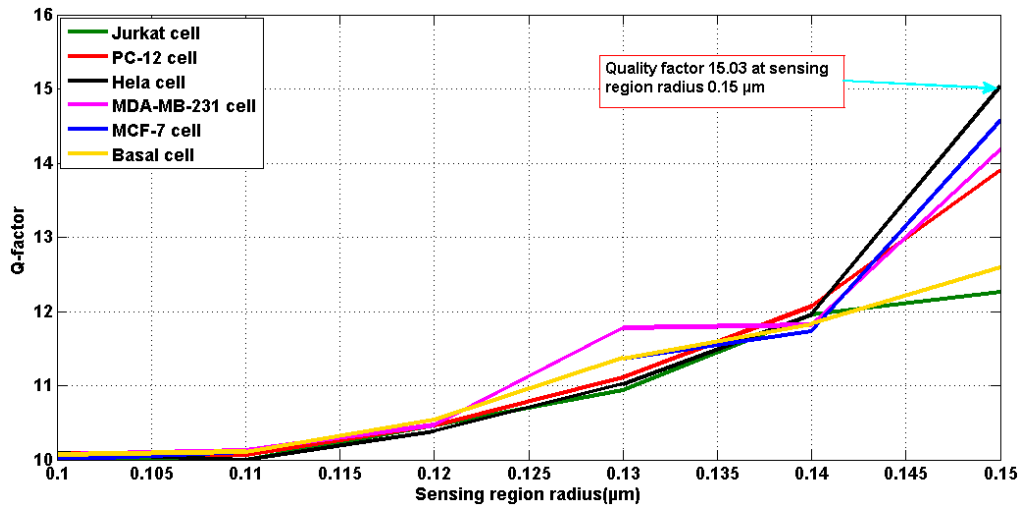


Fig. 6. Quality factor *versus* radius of the sensing region.

is 0.0993 RIU, obtained for detecting skin cancer cells at  $r_s = 0.14 \mu\text{m}$  can be seen in Fig. 7. Moreover, from Fig. 8, we can see that the highest FOM of  $10.07462 \text{ RIU}^{-1}$  is also obtained for detecting skin cancer cells at  $r_s = 0.14 \mu\text{m}$ . Here the quality factor is considerably low; the quality factor takes a maximum value of 10.09 for HeLa normal cell and a minimum value of 9.72 for MDA-MB-231 normal cell.

In Table 2, Some of the biosensors reported from the literature were collected for comparison. Relatively high sensitivity is obtained for the proposed structures.

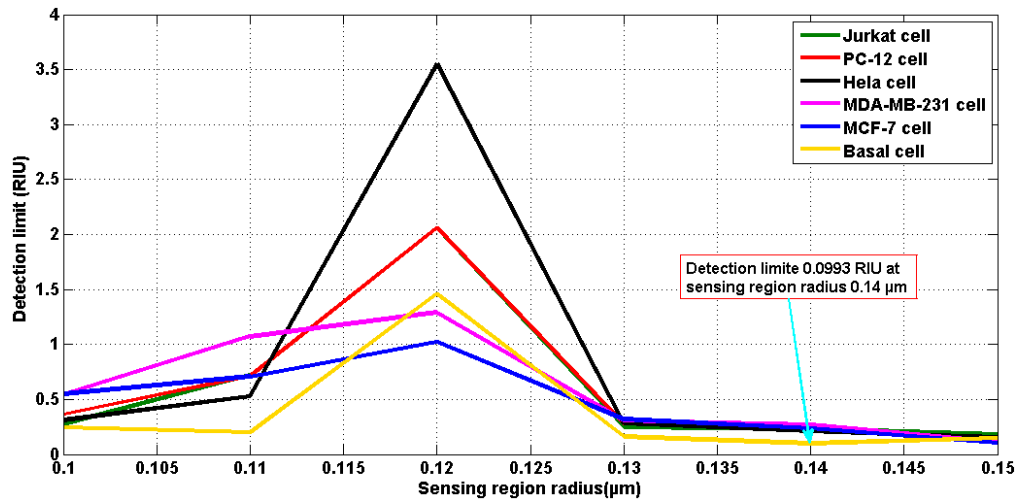


Fig. 7. Detection limit *versus* radius of the sensing region.

Table 1. Comparison of the characteristics of certain 2D-PhC based biosensors.

Reference	Type	Sensitivity [nm/RIU]	Quality factor [RIU]	Detection limit [RIU]	Figure of merit [RIU <sup>-1</sup> ]
[23]	2D photonic crystal slab with ring-shaped holes	636	—	—	—
[24]	Ring resonant cavity coupled waveguide	330	35,517	$1.24 \times 10^{-5}$	8000
[25]	Ring-shaped holes cavity-coupled waveguide	462	$1.11 \times 10^5$	$3.03 \times 10^{-6}$	—
[26]	Two waveguides and a nanocavity	136.6	3915	—	—
[27]	Waveguide surrounded by two rows of RSH <sup>1</sup>	575	7070	—	—
[28]	Ring resonators and bus and drop waveguides	231	4561	$1.29 \times 10^{-4}$	—
[29]	Two waveguide couplers and one micro-cavity	292.46	49.767	—	—
[30]	A waveguide with a nanocavity double holes	410.87	10231.94	—	—
[31]	Two parallel planar waveguide gratings	497.83	—	—	551
[32]	Stampfli-type PQC <sup>2</sup> with concentric ring micro-cavity	613	79423	—	31872
[40]	Surface plasmon polariton biosensor	677	—	—	39
This work	Two waveguides and a nanocavity	1350	15.03	0.0993	10.07462

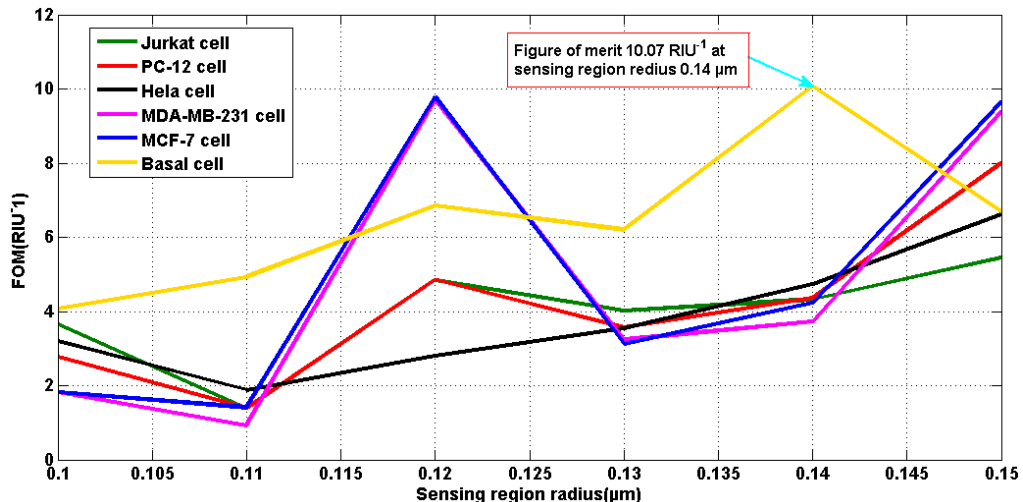


Fig. 8. Figure of merit *versus* radius of the sensing region.

#### 4. Conclusions

By applying the optical properties of photonic crystals, we realize a small-size biosensor based on silicon rods arranged as a square structure in an air background with linear waveguides and one nanocavity to sense cancerous cells. First, the PWE computational method is employed to envisage the photonic band diagram of the proposed structure without defects, and the diagram shows a photonic band gap from  $0.2818a/\lambda$  to  $0.4166a/\lambda$ . Then we use the finite difference time domain method to predict the electromagnetic field distribution in the proposed structure and then plot the transmission spectrum of Gaussian pulse centered at 1550 nm through the biosensor structure in the presence of different cells with different radii. Therefore the detection principle is based on the refractive index change of nanocavity. By binding a cell into the sensing region, we can differentiate a slight change of resonant peak in the output transmission spectrum, which leads to determining if cell cancer is cancerous or benign. Finally, we have proposed applying the optical properties of photonic crystals to realize a small biosensor with an optimum sensing region radius equal to 0.14  $\mu\text{m}$  and characterized by a high sensitivity of 1350 nm/RIU and a low resolution of 0.0993 RIU. The high-quality factor of 15.03 can be achieved for the proposed sensor, which claims the effectiveness of the proposed biosensor. So, with the above-stated sensing principles, the proposed structure can be an apt candidate for cancer cell detection.

#### References

- [1] JOANNOPOULOS J.D., JOHNSON S.G., WINN J.N., MEADE R.D., *Photonic Crystals: Molding the Flow of Light*, Princeton University Press, 2011.
- [2] HO K.M., CHAN C.T., SOUKOULIS C.M., *Existence of a photonic gap in periodic dielectric structures*, Physical Review Letters **65**(25), 1990: 3152-3155. <https://doi.org/10.1103/PhysRevLett.65.3152>

- [3] BERGER V., *From photonic band gaps to refractive index engineering*, Optical Materials **11**(2-3), 1999: 131-142. [https://doi.org/10.1016/S0925-3467\(98\)00039-1](https://doi.org/10.1016/S0925-3467(98)00039-1)
- [4] FENZL C., HIRSCH T., WOLFBEIS O.S., *Photonic crystals for chemical sensing and biosensing*, Angewandte Chemie **53**(13), 2014: 3318-3335. <https://doi.org/10.1002/anie.201307828>
- [5] NAIR R.V., VIJAYA R., *Photonic crystal sensors: An overview*, Progress in Quantum Electronics **34**(3), 2010: 89-134.
- [6] TAYA S.A., SHAHEEN S.A., *Binary photonic crystal for refractometric applications (TE case)*, Indian Journal of Physics volume **92**(4), 2018: 519-527. <https://doi.org/10.1007/s12648-017-1130-z>
- [7] SHAHEEN S.A., TAYA S.A., *Propagation of p-polarized light in photonic crystal for sensor application*, Chinese Journal of Physics **55**(2), 2017: 571-582. <https://doi.org/10.1016/j.cjph.2016.12.005>
- [8] YEO J.C., LIM C.T., *Emerging flexible and wearable physical sensing platforms for healthcare and biomedical applications*, Microsystems & Nanoengineering **2**, 2016: 16043. <https://doi.org/10.1038/micronano.2016.43>
- [9] MALININ A.V., ZANISHEVSKAJA A.A., TUCHIN V.V., SKIBINA Y.S., SILOKHIN I.Y., *Photonic crystal fibers for food quality analysis*, Proceedings of the SPIE, Vol. 8427, Biophotonics: Photonic Solutions for Better Health Care III, 2012: 842746. <https://doi.org/10.1117/12.924096>
- [10] LIU C., ZHANG L., ZHANG X., JIA Y., DI Y., GAN Z., *Bioinspired free-standing one-dimensional photonic crystals with janus wettability for water quality monitoring*, ACS Applied Materials & Interfaces **12**(36), 2020: 40979-40984. <https://doi.org/10.1021/acsmami.0c13618>
- [11] TAYA S.A., SHAHEEN S.A., ALKANOO A.A., *Photonic crystal as a refractometric sensor operated in reflection mode*, Superlattices and Microstructures **101**, 2017: 299-305. <https://doi.org/10.1016/j.spmi.2016.11.057>
- [12] LIU H., LI Z., SHEN R., LI Z., YANG Y., YUAN Q., *Point-of-care pathogen testing using photonic crystals and machine vision for diagnosis of urinary tract infections*, Nano Letters **21**(7), 2021: 2854-2860. <https://doi.org/10.1021/acs.nanolett.0c04942>
- [13] FU F., SHANG L., ZHENG F., CHEN Z., WANG H., WANG J., GU Z., ZHAO Y., *Cells cultured on core-shell photonic crystal barcodes for drug screening*, ACS Applied Materials & Interfaces **8**(22), 2016: 13840-13848. <https://doi.org/10.1021/acsami.6b04966>
- [14] CHOPRA H., KALER R., PAINAM B., *Photonic crystal waveguide-based biosensor for detection of diseases*, Journal of Nanophotonics **10**(3), 2016: 036011. <https://doi.org/10.1117/1.JNP.10.036011>
- [15] TAYA S.A., COLAK I., SUTHAR B., RAMAHI O.M., *Cancer cell detector based on a slab waveguide of anisotropic, lossy, and dispersive left-handed material*, Applied Optics **60**(27), 2021: 8360-8367. <https://doi.org/10.1364/AO.437738>
- [16] BUSWELL S.C., WRIGHT V.A., BURIAK J.M., VAN V., EVOY S., *Specific detection of proteins using photonic crystal waveguides*, Optics Express **16**(20), 2008: 15949-15957. <https://doi.org/10.1364/OE.16.015949>
- [17] SKIVESEN N., CANNING J., KRISTENSEN M., MARTELLI C., TETU A., FRANDSEN L.H., *Photonic crystal waveguide-based biosensor*, Optical Fiber Communication Conference/National Fiber Optic Engineers Conference, OSA Technical Digest (CD), Optica Publishing Group, 2008, paper OTuK2.
- [18] BAYINDIR M., TEMELKURAN B., OZBAY E., BAYINDIR M., TEMELKURAN B., OZBAY E., *Photonic-crystal-based beam splitters*, **77**(24), 2000: 3902-3904. <https://doi.org/10.1063/1.1332821>
- [19] DE VOS K., BARTOLOZZI I., SCHACHT E., BIENSTMAN P., BAETS R., *Silicon-on-Insulator microring resonator for sensitive and label-free biosensing*, Optics Express **15**(12), 2007: 7610-7615. <https://doi.org/10.1364/OE.15.007610>
- [20] CHAO C.Y., FUNG W., GUO L.J., *Polymer microring resonators for biochemical sensing applications*, IEEE Journal of Selected Topics in Quantum Electronics **12**(1), 2006: 134-142. <https://doi.org/10.1109/JSTQE.2005.862945>
- [21] CHAO C.Y., GUO L.J., *Biochemical sensors based on polymer microrings with sharp asymmetrical resonance*, Applied Physics Letters **83**(8), 2003, 1527-1529. <https://doi.org/10.1063/1.1605261>

- [22] SHARMA V., KALYANI V.L., UPADHYAY S., 2017 8th International Conference on Computing, Communication and Networking Technologies (ICCCNT), 2017. <https://doi.org/10.1109/ICCCNT.2017.8204043>
- [23] BOUGRIOU F., BOUCHEMAT T., BOUCHEMAT M., PARAIRE N., *Optofluidic sensor using two-dimensional photonic crystal waveguides*, The European Physical Journal Applied Physics **62**(1), 2013: 11201. <https://doi.org/10.1051/epjap/2013110442>
- [24] HUANG L., TIAN H., YANG D., ZHOU J., LIU Q., ZHANG P., JI Y., *Optimization of figure of merit in label-free biochemical sensors by designing a ring defect coupled resonator*, Optics Communications **332**, 2014: 42-49. <https://doi.org/10.1016/j.optcom.2014.06.033>
- [25] ARAFA S., BOUCHEMAT M., BOUCHEMAT T., BENMERKHI A., HOCINI A., *Infiltrated photonic crystal cavity as a highly sensitive platform for glucose concentration detection*, Optics Communications **384**, 2017: 93-100. <https://doi.org/10.1016/j.optcom.2016.10.019>
- [26] DIVYA J., SELVENDRAN S., SIVANANTHA RAJA A., *Photonic crystal-based optical biosensor: A brief investigation*, Laser Physics **28**(6), 2018: 066206. <https://doi.org/10.1088/1555-6611/aab7d2>
- [27] ANAMORADI A., FASIFI K., *A highly sensitive optofluidic-gas sensor using two dimensional photonic crystals*, Superlattices and Microstructures **125**, 2019: 302-309. <https://doi.org/10.1016/j.spmi.2018.11.019>
- [28] MOHAMMADI M., SEIFOURI M., *Numerical investigation of photonic crystal ring resonators coupled bus waveguide as a highly sensitive platform*, Photonics and Nanostructures - Fundamentals and Applications **34**, 2019: 11-18. <https://doi.org/10.1016/j.photonics.2019.02.002>
- [29] BENMERKHI A., BOUCHEMAT M., BOUCHEMAT T., *Computational study of photonic crystal resonator for biosensor application*, Frequenz **73**(9-10), 2019: 307-316. <https://doi.org/10.1515/freq-2019-0025>
- [30] MOHAMMED N.A., HAMED M.M., KHALAF A.A.M., ALSAYYARI A., EL-RABAIE S., *High-sensitivity ultra-quality factor and remarkable compact blood components biomedical sensor based on nano-cavity coupled photonic crystal*, Results in Physics **14**, 2019: 102478. <https://doi.org/10.1016/j.rinp.2019.102478>
- [31] LU X., ZHENG G.G., ZHOU P., *High performance refractive index sensor with stacked two-layer resonant waveguide gratings*, Results in Physics **12**, 2019: 759-765. <https://doi.org/10.1016/j.rinp.2018.12.048>
- [32] SHI A., GE R., LIU J., *Refractive index sensor based on photonic quasi-crystal with concentric ring microcavity*, Superlattices and Microstructures **133**, 2019: 106198. <https://doi.org/10.1016/j.spmi.2019.106198>
- [33] SIEGEL R.L., MILLER K.D., FUCHS H.E., JEMAL A., *Cancer statistics*, 2022, CA: A Cancer Journal for Clinicians **72**(1), 2022: 7-33. <https://doi.org/10.3322/caac.21708>
- [34] RAMANUJAM N.R., AMIRI I.S., TAYA S.A., OLYAEE S., UDAYAKUMAR R., PASUMPOON PANDIAN A., WILSON K.S.J., MAHALAKSHMI P., YUPAPIN P.P., *Enhanced sensitivity of cancer cell using one dimensional nano composite material coated photonic crystal*, Microsystem Technologies **25**, 2019: 189-196. <https://doi.org/10.1007/s00542-018-3947-6>
- [35] ALMAWGANI A.H.M., DAHER M.G., TAYA S.A., COLAK I., PATEL S.K., RAMAHI O.M., *Highly sensitive nano-biosensor based on a binary photonic crystal for cancer cell detection*, Optical and Quantum Electronics **54**, 2022: 554. <https://doi.org/10.1007/s11082-022-03978-0>
- [36] MIYAN H., AGRAHARI R., GOWRE S.K., MAHTO M., JAIN P.K., *Computational study of a compact and high sensitive photonic crystal for cancer cells detection*, IEEE Sensors Journal **22**(4), 2022: 3298 -3305. <https://doi.org/10.1109/JSEN.2022.3141124>
- [37] PARVIN T., AHMED K., ALATWI A.M., RASHED A.N.Z., *Differential optical absorption spectroscopy -based refractive index sensor for cancer cell detection*, Optical Review **28**(1), 2021: 134-143. <https://doi.org/10.1007/s10043-021-00644-w>
- [38] SHI S., CHEN C., PRATHER D.W., *Plane-wave expansion method for calculating band structure of photonic crystal slabs with perfectly matched layers*, Journal of the Optical Society of America A **21**(9), 2004: 1769-1775. <https://doi.org/10.1364/JOSAA.21.001769>

- [39] BERENGER J.-P., *A perfectly matched layer for the absorption of electromagnetic waves*, Journal of Computational Physics **114**(2), 1994: 185-200.
- [40] GHORBANI S., SADEGI M., ADELPOUR Z., *A highly sensitive and compact plasmonic ring nano-bio-sensor for monitoring glucose concentration*, Laser Physics **30**(2), 2020: 026204. <https://doi.org/10.1088/1555-6611/ab5797>

*Received October 17, 2022  
in revised form November 15, 2022*